Inorganic Chemistry

Article

pubs.acs.org/IC

Graphite Oxide/Metal–Organic Framework (MIL-101): Remarkable Performance in the Adsorptive Denitrogenation of Model Fuels

Imteaz Ahmed, Nazmul Abedin Khan, and Sung Hwa Jhung*

Department of Chemistry and Green-Nano Materials Research Center, Kyungpook National University, Daegu 702-701, Korea

Supporting Information

ABSTRACT: A highly porous metal–organic framework (MOF), MIL-101 (Cr-benzenedicarboxylate), was synthesized in the presence of graphite oxide (GO) to produce GO/MIL-101 composites. The porosity of the composites increased remarkably in the presence of a small amount of GO (<0.5% of MIL-101); however, further increases in GO reduced the porosity. GO also accelerated the synthesis of the MIL-101. The composites (GO/MIL-101) were used, for the first time, in liquid-phase adsorptions. The adsorptive removal of nitrogen-containing compounds (NCCs) and sulfur-containing compounds (SCCs) from model fuels demonstrated the potential applications of the composites in adsorptions, and the adsorption capacity was dependent on the surface area and pore volume of the composites. Most importantly, the GO/MIL-101 composite has the highest adsorption capacity for NCCs among reported adsorbents so far, partly because of the increased porosity of the composite. Finally, the results suggest that GO could be used in the synthesis of highly porous MOF composites, and the obtained materials could be used in various adsorptions in both liquid and gas/vapor phase (such as H_2, CH_4, and CO_2 storage) adsorptions, because of the high porosity and functional GO.

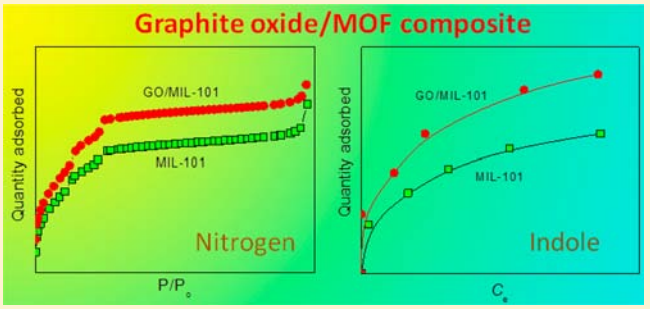

1. INTRODUCTION

Recently, porous materials including metal–organic frameworks (MOFs) or coordination polymers composed of metal ions/clusters and coordinated linkers are one of the most rapidly growing categories of materials.[1−3] The particular interest in MOF materials is because of the easy tunability of their pore size and shape, from a microporous scale to a mesoporous scale, by changing the connectivity of the inorganic moiety and the nature of the organic linkers. MOFs have many applications, including gas adsorption/storage, separation, catalysis, adsorption of organic molecules, drug delivery, luminescence, electrode materials, carriers for nanomaterials, magnetism, polymerization, imaging, and so on.[1−9] MOFs are promising materials for adsorption-related applications, because of the easy modification of their pore surfaces, which leads to the selective adsorption of some specific guest molecules that have particular functional groups.

Although MOF itself shows very promising physical and chemical properties for various applications, its properties can be further improved by modifying or specifying its structure or chemical nature in several ways. These include grafting active groups,[10] changing organic linkers,[11] impregnating suitable active materials[12] and making composites with suitable materials,[13,14] post-synthetic ligand and ion exchange,[15] etc. Among the mentioned modification techniques, the concept of MOF composites is relatively new, and a few reports have been published recently on the successful syntheses and promising applications. A composite is a multicomponent material, with multiple phases, that has at least one continuous phase.[16] By composing MOFs with suitable materials, the synthesis kinetics, morphology, physicochemical properties, and potential applications can be largely improved.[15,17−20] Moreover, the composing procedure is sometimes less energy intensive and relatively easy, compared with the synthesis of the virgin MOFs.[20−22]

One of the successful materials used to prepare MOF composites is graphite oxide (GO). GO is obtained as a laminar material by oxidizing graphite powder with a strong oxidizing agent.[23] Bandosz et al. showed that GO/MOF composites have a large number of newly imparted or improved properties that are usually absent in MOF materials.[23−31] Moreover, GO/MOF composites were successfully used for the gas-phase adsorption of NH_3, NO_2, and H_2S.[23−26,30] They also suggested a possible mechanism for preparing the GO/MOF composites.[14,25−28] It was also found that layers of GO had a structure-directing role in the synthesis of MOFs.[20] However, it is still only an introduction to the syntheses and applications of GO/MOF composites, compared to their vast potential prospects. Therefore, there are ample areas for new research to provide new applications of GO/MOF composites through thorough investigations.

Sulfur-containing compounds (SCCs) and nitrogen-containing compounds (NCCs) from fossil fuels are one of the most

Received: August 5, 2013
Published: December 3, 2013

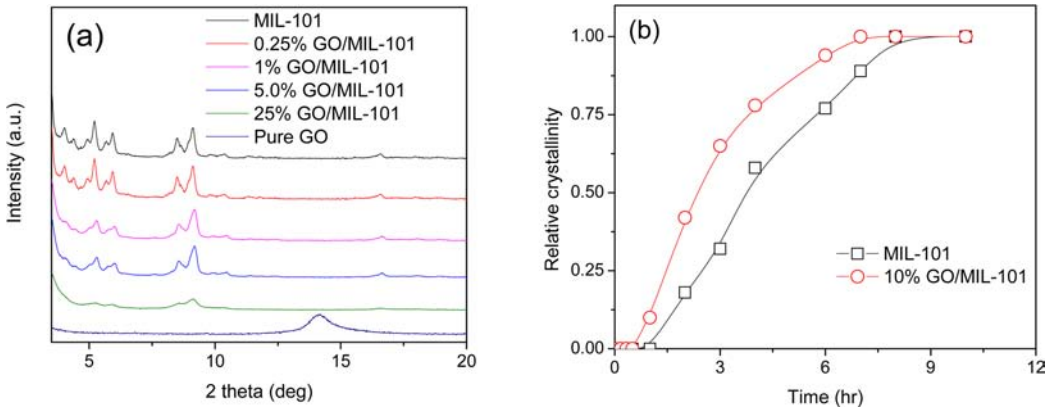

Figure 1. (a) XRD patterns of different GO/MIL-101 (b) Crystallization curves for the synthesis of MIL-101 and 10% GO/MIL-101.

alarming environmental concerns to date. The produced gases upon the combustion of fossil fuel, such as SO_x and NO_x, alter the environment in many different ways. Because of the drastic effects of these materials on the environment throughout the world, governments are becoming stricter on their emissions every day. Because of limited fossil fuels and a large demand for energy, fuels with many contaminants, such as sulfur and nitrogen, and with high viscosity will be utilized over the next several decades.[32−35] Various porous adsorbents, such as activated carbons,[36−39] zeolites,[40] cyclodextrin,[41] and mesoporous materials,[42−49] etc. have been applied to adsorptions, including adsorptive desulfurization (ADS) and adsorptive denitrogenation (ADN). Recently, MOFs[1−3] have attracted considerable attention in the field of the adsorptive removal of hazardous materials[50−56] including ADS[57−64] and ADN[65−68] processes. Maes et al.[65] showed that MOFs, suitably selected and modified, could be used in an ADN and/or ADS process. MIL-101(Cr) had a remarkable adsorption capacity for NCCs and was effective in removing various NCCs.[66,68] To investigate the potential applicability of GO/MOFs, the ADN and ADS of model fuels have been studied.

In this study, detailed synthesis of the GO/MIL-101 material and liquid-phase adsorption, as well as the adsorptive removal of NCCs and SCCs, with those composites, were performed for the first time. It was observed that, upon the inclusion of GO, a faster synthesis of MIL-101 can be obtained. Moreover, a very small amount of GO in MIL-101 is capable of increasing the surface area of MIL-101 by more than 20%. This enhanced surface area can be used to improve the adsorption of NCCs and SCCs accordingly, and GO/MIL-101 has the highest adsorption capacity for NCCs. The applicability of MOF materials can be improved largely by composing MOFs with suitable materials at the appropriate amounts.

2. EXPERIMENTAL SECTION

2.1. Chemicals and Synthesis of Adsorbents. All of the chemicals such as benzothiophene (BT), quinoline (QUI), and indole (IND) utilized in this study were commercial products and used without any further purification. The MOF, MIL-101, used in this study was synthesized as previously described.[69,70] The syntheses were carried out solvothermally by electric heating. Detailed information on the chemicals and MOF synthesis is shown in the Supporting Information.

GO was prepared by a reported method,[71] and the detailed synthesis procedure is as follows: 2 g of graphite powder, 1 g of $NaNO_3$, and 46 mL of concentrated H_2SO_4 were mixed by stirring in a 250-mL beaker situated in an ice bath. Then, 6 g of $KMnO_4$ was added slowly to the mixture. The mixtures were always kept below 20 °C. The ice bath then was removed and the temperature of the mixture was increased up to 35 °C and maintained for 45 min. Then, 100 mL of water was added slowly to the mixture. After that, 100 mL of 3% H_2O_2 was added to the reaction mixture and further stirred for ∼30 min at 80 °C. Finally, a brownish product was washed with 1 M HCl and deionized water, filtered, and dried.

To synthesize the GO/MIL-101 composites, GO was introduced at a specific amount in the precursor mixtures of the MOF. The rest of the synthesis procedure is the same as the synthesis of MIL-101. GO/MIL-101 composites were denoted as *n*% GO/MIL-101, where *n* is the weight percentage of GO used in the reaction mixture, compared with the total weight of the precursors of MIL-101. The actual GO content in the composites was measured by selectively dissolving the MOF portion in 1 M NaOH solution. The insoluble GO was separated from liquid part by centrifugation, washing and drying. GO then was weighed and compared with the weight of the composite. The actual content of GO has been found to be 0.37%, 0.68%, 1.28%, and 15.3% for 0.25%, 0.50%, 1.0%, and 10.0% GO/MIL-101 respectively.

2.2. Characterization. The powder X-ray diffraction (XRD) patterns were obtained with a diffractometer (Model D2 Phaser, Bruker), using Cu Kα radiation. The nitrogen adsorptions of the adsorbents were obtained at a temperature of −196 °C, using a surface area and porosity analyzer (Micromeritics, Model Tristar II 3020) after evacuation at 150 °C for 12 h. The Fourier transform infrared (FT-IR) spectra were recorded with a resolution of 2.0 cm^{-1} on a Jasco Model FTIR-4100 device equipped with an attenuated total reflectance (ATR) accessory. The morphology of the materials was analyzed via scanning electron microscopy (SEM) (Hitachi, Model S-4300). The thermogravimetric analysis (TGA) pattern was obtained with a thermal analyzer system (Seiko, Models TG320 and SSC5200H) under nitrogen flow with a temperature ramping rate of 10 °C min^{-1}.

2.3. General Procedures for the Adsorption Experiments. Stock solutions (10 000 ppm each) for a model fuel were prepared separately for three adsorbates (BT, QUI, and IND) by dissolving them in a mixture of 75 vol % *n*-octane and 25 vol % *p*-xylene. Combined solutions of different concentrations were prepared by successive dilution and mixing of the three solutions. A solution with a fixed concentration of NCCs and SCCs (300 ppm QUI, 300 ppm IND, and 600 ppm BT) was used to determine the adsorption capacity with various adsorption times. Solutions with various concentrations of BT (600−2400 ppm), QUI (300−1200 ppm), and IND (300−1200 ppm) were used to obtain the adsorption isotherms. For the individual adsorption of BT, a stock solution of 10 000 ppm was prepared by dissolving it in *n*-octane only. Then, this solution was diluted up to 1000 ppm BT and used for the individual adsorption experiments of BT.

Before adsorption, the adsorbents were dried in a vacuum oven at 150 °C for 12 h and kept in a desiccator. For every adsorption experiment, an exact amount of the adsorbents (∼5.0 mg) was put in

dx.doi.org/10.1021/ic402012d | *Inorg. Chem.* 2013, 52, 14155−14161

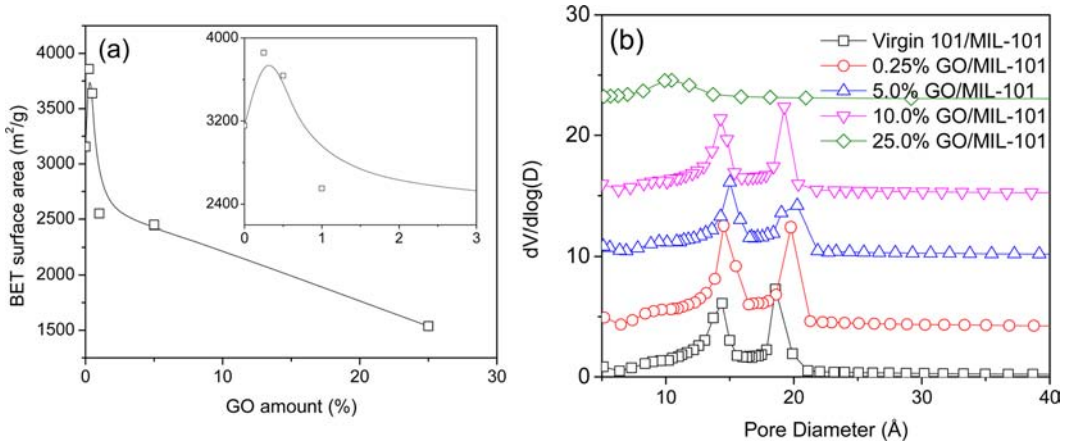

Figure 2. (a) Effect of GO content on the BET surface area of GO/MIL-101 composites; the inset shows an enlarged view of the same graph for small amounts of GO. (b) Pore size distribution curves for MIL-101 and various GO/MIL-101s.

the model fuel solution (~5.0 mL) and shaken for a predetermined time (between 30 min and 12 h) and the adsorption temperature was maintained at 25 °C. After adsorption, the solution was separated from the solid with a syringe filter (PTFE, hydrophobic, 0.5 μm) and analyzed with a GC (DS Science, IGC 7200) equipped with a flame ionization detection (FID) device. The maximum adsorption capacity (Q_0) was calculated with the Langmuir adsorption isotherm. More details on the adsorption isotherms and the method used to get the maximum adsorption capacities are described in the Supporting Information.

After the first run of adsorption with the fresh adsorbent, the used 0.25% GO/MIL-101 was regenerated by washing it with several organic solvents. For this, 0.1 g of filtered adsorbent was immersed in 30 mL of solvent and kept in a sonification bath for 2 h. After that, the composite was filtered and the operation was performed one more time. The adsorbent then was dried in a vacuum oven and the adsorption operations were carried out as previously described. Adsorptions with regenerated composites were repeated up to the fourth run.

3. RESULTS AND DISCUSSION

3.1. Synthesis Kinetics. Figure 1a shows the XRD patterns of the MIL-101s synthesized with different amounts of GO, along with pure GO. The XRD pattern of crystalline GO was not observed in the GO/MIL-101s, which is probably because of the separation in the layers and exfoliation of the GO in the presence of water during the synthesis of the composites.[26,72] In addition, the XRD peaks were quite similar to the patterns of MIL-101 for all the composites, although a lower intensity was observed for a high amount of GO, because of the low concentration of MIL-101. FT-IR data also showed a GO peak only for the high GO/MIL-101 (see Figure S1 in the Supporting Information). The SEM images (see Figure S2 in the Supporting Information) show uniform crystal structures for all the materials; however, comparatively smaller-sized crystals were obtained for the higher amounts of GO in the composite materials. The TGA profiles (see Figure S3 in the Supporting Information) also show a similar thermal stability of the virgin and composite MOFs. At the very beginning, weight loss was observed up to 85 °C, because of the loss of moisture. After that, all the materials were stable up to ~350 °C, because no noticeable weight loss was observed during this period. A gradual weight loss and disintegration of the materials were observed beyond a temperature of 350 °C.

Several methods have been tried to accelerate the synthesis of MOF materials,[17,73] because rapid syntheses have various advantages; microwave- and ultrasound-assisted syntheses are the most prominent among them.[74,75] Figure 1b shows the relative crystallinity of virgin MIL-101 and 10% GO/MIL-101 obtained from the XRD data with different times. An accelerated synthesis of GO/MIL-101, compared to the virgin MOF, was observed, similar to the accelerated syntheses of rectangular MOFs such as Cu-BTC and MOF-5, by composite formation with suitable materials.[21] According to Bandosz and co-workers, GO contains some epoxy groups in their structure, which links with the metal sites of the MOF during composite formation.[27] These epoxy groups act as H_2O molecules, which usually make coordination with the central metal ions of MOFs. Hydrogen boding between the H-atom from the hydroxyl groups of the GO sheets and the O-atom from the chromium oxide octahedra of the MIL-101 also occurs in parallel.[14] Different functional groups, especially epoxy groups, combine with the central metal ions by the removal of H_2O molecules which form a strong GO-MOF interaction.[27] Other functional groups—especially carboxylic or sulfonic groups—are normally formed at the edge of the GO sheets, which also combine with the metal sites of MOFs.[27] So far, it has been reported that spherical MOFs such as MIL-100 and MIL-101 are not easy to be composed with a high concentration of GO, because of the attachment of the GO sheets in various orientations.[26] However, in this study, we confirmed the beneficial role of GO, even at high concentrations, in the rapid synthesis of MIL-101. The chemical affinity of GO and MOF might improve the synthesis kinetics of the MOF, compared to the virgin MIL-101. Therefore, a shorter crystallization time may be observed through the clinging of the MOF nuclei to the GO sheets which propels faster crystallization. As observed, at the very beginning, the crystallization of the GO/MOF composites was faster, compared with the virgin one, suggesting rapid syntheses of various MOFs in the presence of suitable additives such as GO.

3.2. Textural Properties and Characteristics of the GO/MIL-101 Composites. Figure 2a shows the BET surface areas, derived from the N_2 adsorption isotherms shown in Figure S4 in the Supporting Information, of the different composites with different amounts of GO in the syntheses of GO/MIL-101. As mentioned earlier, the epoxy groups of GO act as H_2O molecules, which usually coordinate with the central metal ions of the MOFs. During the linking procedure, delamination of the GO layers might occur, which unveils additional surface area to the composites, especially for

dx.doi.org/10.1021/ic402012d | Inorg. Chem. 2013, 52, 14155−14161

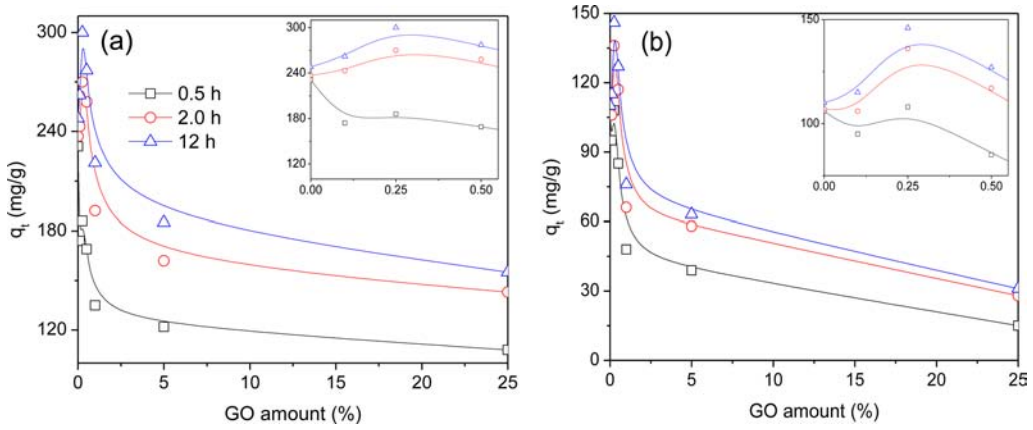

Figure 3. Effect of GO amount of GO/MIL-101 composites on the adsorption of (a) QUI and (b) IND. The hydrocarbon solutions initially contain 600 ppm BT, 300 ppm QUI, and 300 ppm IND. Insets show the enlarged figures in low GO amounts.

composites with a low GO content.[14] It was also reported that a high content of GO was not suitable for spherical caged MOF structures such as MIL-101 or MIL-100, because of the capability of the GO sheets to attach in various orientations.[26] In this case, the differently oriented GO sheets may hamper further attachment of the GO sheets over the MOF cages. Therefore, for MIL-101 type materials, a very low content of GO would be much more helpful in producing a successful composite different from a composite with a high GO content.[76] Moreover, complete delamination cannot occur with a high GO content; therefore, it cannot contribute to the enhancement of the surface area.[27] This could be the reason why low-porosity GO/MIL-101 is obtained with high GO contents.[76] Because of the graphene layers (individual layers of GO), separation of the MIL-101 cages might occur by the attachment of the GO layers, which provide additional surface areas to the composites. Accordingly, as shown in Figure 2a, the BET surface area was maximum with a GO content of 0.25%; however, the surface area was lower in the materials with a higher GO content, because of the low contribution of GO to the surface area. The pore size distribution (Figure 2b) also implied an intact MIL-101 cage structure for the GO/MIL-101 composites when the content was up to 10%. The lack of distribution of the additional pores, even in the presence of GO, could be due to the randomness of the newly created pores.

3.3. Adsorption Experiments. Because QUI, IND, and their derivatives are found as major NCC impurities in fuels, they were used as the representatives of basic and neutral NCCs, respectively, to mimic the composition of fossil fuels. In addition, BT and its derivatives are the prominent SCCs in commercial crude oils. Therefore, BT was added along with QUI and IND into the model fuel as a representative of SCCs. The solvent for the model fuel was comprised of 75% *n*-octane and 25% *p*-xylene, to simulate commercial fuels, since they contain nearly 25% aromatics.

The effect of the GO amount on the adsorbed capacity of QUI and IND and detailed kinetic curves are shown in Figure 3 and Figure S5 in the Supporting Information, respectively. The kinetics data of Figure S5 suggest a rapid adsorption of QUI and IND over the virgin MIL-101, similar to previous reports.[65,68] However, GO/MIL-101 composites, compared with the virgin MIL-101, showed very low adsorption kinetics. As shown in Table S1 in the Supporting Information, the kinetic constants over GO/MIL-101 were $\sim^1/_8$ to $\sim^1/_{11}$ of that over the virgin MIL-101. Despite the low kinetics, the adsorption capacity of the composites (GO/MIL-101 with 0.1%−0.5% GO) was higher than that of the virgin MIL-101. In fact, compared to all the previous reports, the 0.25% GO/MIL-101 material has the best performance for ADN (see below). Therefore, it can be suggested that GO has a favorable effect on the adsorption of NCCs and SCCs, even though it has a retarding effect for the diffusion of the adsorbates through the adsorbents (GO/MIL-101s). The increase in adsorption can be attributed to the increase in surface area, because the correlation of the adsorption amount of QUI and IND was nearly a perfect proportional fit with the surface area of the adsorbents (see Figure 4). The adsorption experiments were

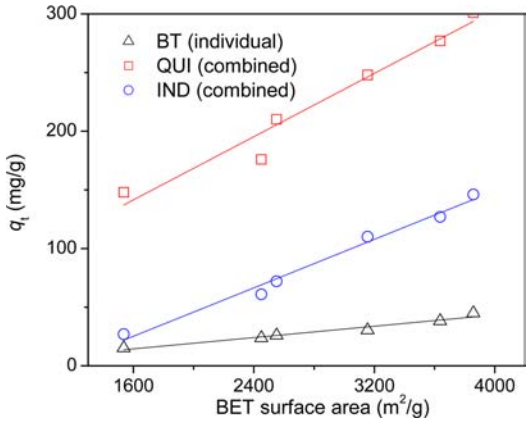

Figure 4. Effect of BET surface area of GO/MIL-101 (different surface areas were obtained with different GO content) on the adsorbed amounts for different adsorbates BT, QUI, and IND.

also carried out for a physical mixture of 0.25% GO and MIL-101. As shown in Figure S5 in the Supporting Information, the physical mixture, however, showed poor performance (compared with GO/MIL-101 or MIL-101) in adsorption, because of negligible adsorption of the GO. In a combined system, BT was negligibly adsorbed (see Figures S5 and S6(a) in the Supporting Information) on the adsorbents used in this study, because NCCs are preferably adsorbed, compared with SCCs.[40,67] Therefore, the BT adsorption experiments were continued for an individual system containing only BT as the adsorbate (1000 ppm) in order to obtain a good experimental outcome (Figure 5). After completing the separate experiments,

dx.doi.org/10.1021/ic402012d | *Inorg. Chem.* 2013, 52, 14155−14161

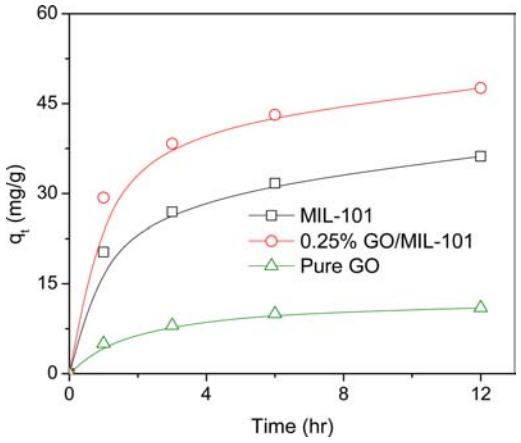

Figure 5. Individual adsorption of BT over virgin MIL-101 and 0.25% GO/MIL-101 (only BT was added in *n*-octane).

it was determined that BT also shows a linear correlation for adsorption with the surface area of the composites (see Figure 4). Even though it has been reported that porosity and functional groups are important for gas- and liquid-phase adsorptions, respectively,[38] porosity is also very important for liquid-phase adsorption, which is in agreement with earlier studies.[52,53] The adsorption experiments were further done for the 0.25% GO/MIL-101 because it exhibited the maximum adsorption, and the adsorption capacities at equilibrium were compared with those over the virgin MIL-101 (see Figure 6, as well as Figure S6(b) in the Supporting Information). The adsorption results were fitted with the Langmuir equations (see Figure S7 in the Supporting Information), and the maximum adsorption capacities (Q_0) were calculated. Table 1 shows the maximum adsorption capacities of the virgin MIL-101 and 0.25% GO/MIL-101, along with the surface areas. The surface area of 0.25% GO/MIL-101 was higher than that of the MIL-101 by 22%. Accordingly, the Q_0 value of QUI and IND also increased by 24% and 30%, respectively, in the 0.25% GO/MIL-101. Table 2 compares the adsorption capacities of NCCs over various adsorbents, including GO/MIL-101. Even though the adsorption conditions are not exactly the same from one adsorbent to another, it can be concluded that the adsorption capacity of GO/MIL-101 in this study is the highest among the various adsorbents that have been reported so far.

Table 1. Physiochemical Properties and the Maximum Adsorption Capacities of MIL-101 and 0.25% GO/MIL-101

adsorbent	BET surface area (m^2/g)	total pore volume (cm^3/g)	adsorbate	Q_0 (mg/g)	Q_0 (cm^3/g)	total Q_0 (cm^3/g)
MIL-101	3155	1.89	BT	18.3	0.02	0.65
			QUI	481	0.44	
			IND	244	0.19	
0.25% GO/MIL-101	3858	2.09	BT	28.2	0.03	0.79
			QUI	549	0.50	
			IND	319	0.26	

Table 2. Maximum Adsorption Capacities (Q_0) for NCCs over Different Adsorbents

adsorbent	type of NCCs	Q_0 (mg_{NCC}/g)	Q_0 (mg_N/g)	ref
AC	quinoline, indole		39.0	76
Cu–Y	NCCs with aromatic rings		3.0	39
silica-zirconia Cogel	mixed		10.0	77
AC	quinoline, indole		18.4	78
alumina	quinoline, indole		7.16	
meso-silica	mixed		8.14	79
AC	mixed		17.6	37
AC	quinoline, indole, carbazole		51.9	80
MOF (MIL-101)	mixed		19.6	65
MOFs	indoles, carbazoles		16.0	64
MIL-100 (Cr)	quinoline, indole	445	49.4	66
PWA/MIL-101	quinoline, indole	426	47.8	67
GO/MIL-101	quinoline, indole	863	97.6	this work

3.4. Reusability of an Adsorbent. Because commercial applications of an adsorptive removal may rely on the reusability of an adsorbent, the reusability of the 0.25% GO/MIL-101 was also studied after solvent-washing of the used MOF. So far, several solvents with various polarities (such as toluene,[12,39] methylisobutyl ketone,[82] ethanol,[50] and acetone[66]) have been used to reactivate spent adsorbents in different

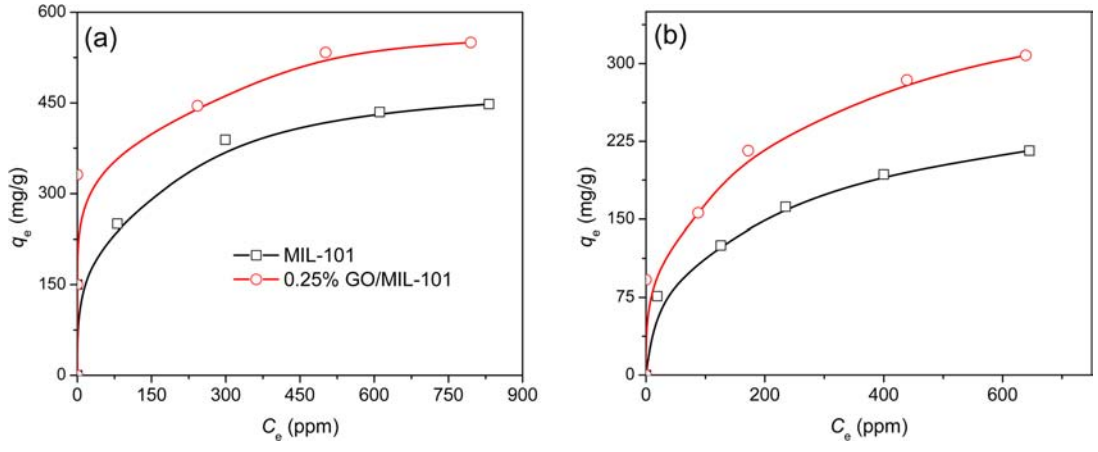

Figure 6. Adsorption isotherms for (a) QUI and (b) IND over MIL-101 and 0.25% GO/MIL-101.

dx.doi.org/10.1021/ic402012d | *Inorg. Chem.* 2013, 52, 14155–14161

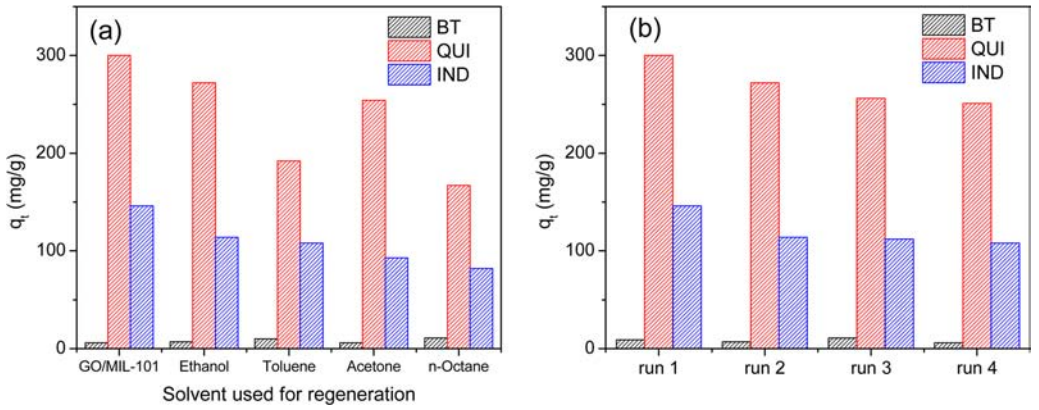

Figure 7. (a) Effect of solvents applied in the regeneration of the used 0.25% GO/MIL-101 on the adsorptive removal of BT, QUI, and IND. (b) Effect of regeneration cycles on the performances of adsorptive removal of BT, QUI, and IND over regenerated 0.25% GO/MIL-101 by washing with ethanol (run 1 is represents the fresh adsorbent). The hydrocarbon solutions containing 600 ppm BT, 300 ppm QUI, and 300 ppm IND.

studies. Figure 7 shows the effect of solvent washing on the adsorption result. The performance of the used 0.25%GO/MIL-101 after solvent washing was dependent on the used solvent, and the reusability of the material for QUI decreased in the order of

ethanol > acetone > toluene > *n*-octane

washing (see Figure 7a). For IND, adsorption decreased in the following order:

ethanol > toluene > acetone > *n*-octane

(Figure 7a). Therefore, ethanol was used to wash the used adsorbent for the next runs of adsorption because both of the NCCs showed the highest adsorption after ethanol washing. Figure 7b shows that, up to the fourth run, the performance of the adsorption remained good (even with a slight reduction in adsorption quantity), confirming the applicability of the GO/MIL-101 composites in the adsorptive removal of NCCs and SCCs.

4. CONCLUSION

The composing of metal−organic frameworks (MOFs) with suitable materials can improve their properties as well as the applicability of MOFs to a large extent. In this study, composites of the graphite oxide/metal organic framework (MIL-101) have been successfully prepared, and the synthesis kinetics can also be improved by composing MIL-101 with GO. The surface area of the composites was greatly dependent on the amount of GO, and a small amount (typically 0.25%) of GO content improved the surface area of the MIL-101 remarkably. We have demonstrated, for the first time, that the adsorption capacities of GO/MIL-101 (with a suitable GO content) for nitrogen-containing compounds (NCCs) and sulfur-containing compounds (SCCs) were remarkably enhanced when preparing composites with GO, because of the increased porosity of the composites. Therefore, the composite has the highest adsorption capacity for NCCs among the reported adsorbents so far. It was also found that the adsorbent could be used several times after regeneration without noticeable degradation in performance. This improved surface area or adsorption capacity suggests a wide range of applications of the composites in adsorption, catalysis, separation, drug delivery, and so on.

■ ASSOCIATED CONTENT

Supporting Information

Supporting Information for synthesis and characterization, as well as detailed adsorption data, is available. This material is available free of charge via the Internet at http://pubs.acs.org.

■ AUTHOR INFORMATION

Corresponding Author

*Fax: 82-53-950-6330. E-mail: sung@knu.ac.kr.

Notes

The authors declare no competing financial interest.

■ ACKNOWLEDGMENTS

This work was supported by a National Research Foundation of Korea (NRF) grant funded by the Korea government (MSIP) (Grant No. 2013R1A2A2A01007176).

■ REFERENCES

(1) Férey, G. *Chem. Soc. Rev.* **2008**, *37*, 191−214.
(2) Kitagawa, S.; Kitaura, R.; Noro, S.-I. *Angew. Chem., Int. Ed.* **2004**, *43*, 2334−2375.
(3) Yaghi, O. M.; O'Keeffe, M.; Ockwig, N. W.; Chae, H. K.; Eddaoudi, M.; Kim, J. *Nature* **2003**, *423*, 705−714.
(4) Czaja, A. U.; Trukhan, N.; Müller, U. *Chem. Soc. Rev.* **2009**, *38*, 1284−1293.
(5) Meek, S. T.; Greathouse, J. A.; Allendorf, M. D. *Adv. Mater.* **2011**, *23*, 249−267.
(6) Wu, H.; Gong, Q.; Olson, D. H.; Li, J. *Chem. Rev.* **2012**, *112*, 836−868.
(7) Li, J.-R.; Sculley, J.; Zhou, H.-C. *Chem. Rev.* **2012**, *112*, 869−932.
(8) Horcajada, P.; Gref, R.; Baati, T.; Allan, P. K.; Maurin, G.; Couvreur, P.; Férey, G.; Morris, R. E.; Serre, C. *Chem. Rev.* **2012**, *112*, 1232−1268.
(9) Kitagawa, S.; Matsuda, R. *Coord. Chem. Rev.* **2007**, *251*, 2490−2509.
(10) Hwang, Y. K.; Hong, D.-Y.; Chang, J.-S.; Jhung, S. H.; Seo, Y.-K.; Kim, J.; Vimont, A.; Daturi, M.; Serre, C.; Férey, G. *Angew. Chem., Int. Ed.* **2008**, *47*, 4144−4148.
(11) Eddaoudi, M.; Kim, J.; Rosi, N.; Vodak, D.; Wachter, J.; O'Keeffe, M.; Yaghi, O. M. *Science* **2002**, *295*, 469−472.
(12) Thornton, A. W.; Nairn, K. M.; Hill, J. M.; Hill, A. J.; Hill, M. R. *J. Am. Chem. Soc.* **2009**, *131*, 10662−10669.
(13) Yang, S. J.; Choi, J. Y.; Chae, H. K.; Cho, J. H.; Nahm, K. S.; Park, C. R. *Chem. Mater.* **2009**, *21*, 1893−1897.
(14) Petit, C.; Bandosz, T. J. *Adv. Mater.* **2009**, *21*, 4753−4757.

(15) Kim, M.; Cahill, J. F.; Fei, H.; Prather, K. A.; Cohen, S. M. *J. Am. Chem. Soc.* **2012**, *134*, 18082−18088.
(16) Work, W. J.; Horie, K.; Hess, M.; Stepto, R. F. T. *Pure Appl. Chem.* **2004**, *76*, 1985−2007.
(17) Stock, N.; Biswas, S. *Chem. Rev.* **2012**, *112*, 933−969.
(18) O'Neill, L. D.; Zhang, H.; Bradshaw, D. *J. Mater. Chem.* **2010**, *20*, 5720−5726.
(19) Ostermann, R.; Cravillon, J.; Weidmann, C.; Wiebcke, M.; Smarsly, B. M. *Chem. Commun.* **2011**, *47*, 442−444.
(20) Jahan, M.; Bao, Q.; Yang, J.-X.; Loh, K. P. *J. Am. Chem. Soc.* **2010**, *132*, 14487−14495.
(21) Wee, L. H.; Bajpe, S. R.; Janssens, N.; Hermans, I.; Houthoofd, K.; Kirschhock, C. E. A.; Martens, J. A. *Chem. Commun.* **2010**, *46*, 8186−8188.
(22) Wee, L. H.; Janssens, N.; Bajpe, S. R.; Kirschhock, C. E. A.; Martens, J. A. *Catal. Today* **2011**, *171*, 275−280.
(23) Petit, C.; Bandosz, T. J. *Adv. Funct. Mater.* **2011**, *21*, 2108−2117.
(24) Petit, C.; Mendoza, B.; Bandosz, T. J. *ChemPhysChem* **2010**, *11*, 3678−3684.
(25) Seredych, M.; Bandosz, T. J. *Langmuir* **2010**, *26*, 4591−4598.
(26) Petit, C.; Bandosz, T. J. *Dalton Trans.* **2012**, *41*, 4027−4035.
(27) Petit, C.; Burress, J.; Bandosz, T. J. *Carbon* **2011**, *49*, 563−572.
(28) Seredych, M.; Bandosz, T. J. *J. Phys. Chem. C* **2007**, *111*, 15596−15604.
(29) Petit, C.; Huang, L.; Jagiello, J.; Kenvin, J.; Gubbins, K. E.; Bandosz, T. J. *Langmuir* **2011**, *27*, 13043−13051.
(30) Petit, C.; Mendoza, B.; O'Donnell, D.; Bandosz, T. J. *Langmuir* **2011**, *27*, 10234−10242.
(31) Levasseur, B.; Petit, C.; Bandosz, T. J. *ACS Appl. Mater. Interfaces* **2010**, *12*, 3606−3613.
(32) Srivastava, V. C. *RSC Adv.* **2012**, *2*, 759−783.
(33) Pawelec, B.; Navarro, R. M.; Campos-Martin, J. M.; Fierro, J. L. G. *Catal. Sci. Technol.* **2011**, *1*, 23−42.
(34) Stanislaus, A.; Marafi, A.; Rana, M. S. *Catal. Today* **2010**, *153*, 1−68.
(35) Samokhvalov, A.; Tatarchuk, B. J. *Catal. Rev. Sci. Eng.* **2010**, *52*, 381−410.
(36) Seredych, M.; Deliyanni, E.; Bandosz, T. J. *Fuel* **2010**, *89*, 1499−1507.
(37) Hernandez, S. P.; Fino, D.; Russo, N. *Chem. Eng. Sci.* **2010**, *65*, 603−609.
(38) Almarri, M.; Ma, X.; Song, C. *Energy Fuel* **2009**, *23*, 3940−3947.
(39) Almarri, M.; Ma, X.; Song, C. *Ind. Eng. Chem. Res.* **2009**, *48*, 951−960.
(40) Hernndez-Maldonado, J.; Yang, R. T. *Angew. Chem., Int. Ed.* **2004**, *43*, 1004−1006.
(41) Song, X.-L.; Sun, L.-B.; He, G.-S.; Liu, X.-Q. *Chem. Commun.* **2011**, *47*, 650−652.
(42) Yin, Y.; Jiang, W.-J.; Liu, X.-Q.; Li, Y.-H.; Sun, L.-B. *J. Mater. Chem.* **2012**, *22*, 18514−18521.
(43) Sang, L.-C.; Vinu, A.; Coppens, M.-O. *Langmuir* **2011**, *27*, 13828−13837.
(44) Ariga, K.; Vinu, A.; Ji, Q.; Ohmori, O.; Hill, J. P.; Acharya, S.; Koike, J.; Shiratori, S. *Angew. Chem., Int. Ed.* **2008**, *47*, 7254−7257.
(45) Tian, W.-H.; Sun, L.-B.; Song, X.-L.; Liu, X.-Q.; Yin, Y.; He, G.-S. *Langmuir* **2010**, *26*, 17398−17404.
(46) Ji, Q.; Yoon, S. B.; Hill, J.; Vinu, A.; Yu, J.-S.; Ariga, K. *J. Am. Chem. Soc.* **2009**, *131*, 4220−4221.
(47) Ren, Y.; Ma, Z.; Bruce, P. G. *Chem. Soc. Rev.* **2012**, *41*, 4909−4927.
(48) Yang, P.; Gai, S.; Lin. *J. Chem. Soc. Rev.* **2012**, *41*, 3679−3698.
(49) Ariga, K.; Vinu, A.; Yamauchi, Y.; Ji, Q.; Hill, J. P. *Bull. Chem. Soc. Jpn.* **2012**, *1*, 1−32.
(50) Zhang, H.; Li, G.; Jia, Y.; Liu, H. *J. Chem. Eng. Data* **2010**, *55*, 173−177.
(51) Jhung, S. H.; Khan, N. A.; Hasan, Z. *CrystEngComm* **2012**, *14*, 7099−7109.
(52) Hasan, Z.; Jeon, J.; Jhung, S. H. *J. Hazard. Mater.* **2012**, *209−210*, 151−157.
(53) Haque, E.; Lee, J. E.; Jang, I. T.; Hwang, Y. K.; Chang, J.-S.; Jegal, J.; Jhung, S. H. *J. Hazard. Mater.* **2010**, *181*, 535−542.
(54) Haque, E.; Jun, J. W.; Jhung, S. H. *J. Hazard. Mater.* **2011**, *185*, 507−511.
(55) Khan, N. A.; Hasan, Z.; Jhung, S. H. *J. Hazard. Mater.* **2013**, *244−245*, 444−456.
(56) Khan, N. A.; Hasan, Z.; Jhung, S. H. *Adv. Porous Mater.* **2013**, *1*, 91−102.
(57) Khan, N. A.; Jhung, S. H. *Angew. Chem., Int. Ed.* **2012**, *51*, 1198−1201.
(58) Khan, N. A.; Jun, J. W.; Jeong, J. H.; Jhung, S. H. *Chem. Commun.* **2011**, *47*, 1306−1308.
(59) Khan, N. A.; Jhung, S. H. *Fuel Process. Technol.* **2012**, *100*, 49−54.
(60) Cychosz, K. A.; Wong-Foy, A. G.; Matzger, A. J. *J. Am. Chem. Soc.* **2009**, *131*, 14538−14543.
(61) Khan, N. A.; Jhung, S. H. *J. Hazard. Mater.* **2012**, *237−238*, 180−185.
(62) Achmann, S.; Hagen, G.; Hämmerle, M.; Malkowsky, I. M.; Kiener, C.; Moos, R. *Chem. Eng. Technol.* **2010**, *33*, 275−280.
(63) Blanco-Brieva, G.; Campos-Martin, J. M.; Al-Zahrani, S. M.; Fierro, J. L. G. *Fuel* **2011**, *90*, 190−197.
(64) Blanco-Brieva, G.; Campos-Martin, J. M.; Al-Zahrani, S. M.; Fierro, J. L. G. *Global NEST J.* **2010**, *12*, 296−304.
(65) Maes, M.; Trekels, M.; Boulhout, M.; Schouteden, S.; Vermoortele, F.; Alaerts, L.; Heurtaux, D.; Seo, Y.-K.; Hwang, Y. K.; Chang, J.-S.; Beurroies, I.; Denoyel, R.; Temst, K.; Vantomme, A.; Horcajada, P.; Serre, C.; De Vos, D. E. *Angew. Chem., Int. Ed.* **2011**, *50*, 4210−4214.
(66) Nuzhdin, A. L.; Kovalenko, K. A.; Dybtsev, D. N.; Bukhtiyarova, G. A. *Mendeleev Commun.* **2010**, *20*, 57−58.
(67) Ahmed, I.; Hasan, Z.; Khan, N. A.; Jhung, S. H. *Appl. Catal., B: Environ.* **2013**, *129*, 123−129.
(68) Ahmed, I.; Khan, N. A.; Hasan, Z.; Jhung, S. H. *J. Hazard. Mater.* **2013**, *250−251*, 37−44.
(69) Férey, G.; Mellot-Draznieks, C.; Serre, C.; Millange, F.; Dutour, J.; Surblé, S.; Mirgiolaki, I. *Science* **2005**, *309*, 2040−2042.
(70) Khan, N. A.; Jhung, S. H. *Crystal Growth Des.* **2010**, *10*, 1860−1865.
(71) Han, D.; Yan, L.; Chen, W.; Li, W. *Carbohydr. Polym.* **2011**, *83*, 653−658.
(72) Park, S.; Ruoff, R. S. *Nat. Nanotechnol.* **2009**, *4*, 217−224.
(73) Kuppler, R. J.; Timmons, D. J.; Fang, Q.-R.; Li, J.-R.; Makal, T. A.; Young, M. D.; Yuan, D.; Zhao, D.; Zhuang, W.; Zhou, H.-C. *Coord. Chem. Rev.* **2009**, *253*, 3042−3066.
(74) Klinowski, J.; Paz, F. A. A.; Silva, P.; Rocha, J. *Dalton Trans.* **2011**, *40*, 321−330.
(75) Haque, E.; Khan, N. A.; Park, J. H.; Jhung, S. H. *Chem.—Eur. J.* **2010**, *16*, 1046−1052.
(76) Liu, X.; Zhou, H.; Zhang, Y.; Liu, Y.; Yuan, A. *Chin. J. Chem.* **2012**, *30*, 2563−2566.
(77) Sano, Y.; Choi, K.-H.; Korai, Y.; Mochida, I. *Appl. Catal. B: Environ.* **2004**, *49*, 219−225.
(78) Bae, Y.-S.; Kim, M.-B.; Lee, H.-J.; Lee, C.-H.; Ryu, J. W. *AIChE J.* **2006**, *52*, 510−521.
(79) Kim, J. H.; Ma, X.; Zhou, A.; Song, C. *Catal. Today* **2006**, *111*, 74−83.
(80) Kwon, J.-M.; Moon, J.-H.; Bae, Y.-S.; Lee, D.-G.; Sohn, H.-C.; Lee, C.-H. *ChemSusChem* **2008**, *1*, 307−309.
(81) Wen, J.; Han, X.; Lin, H.; Zheng; Chu, W. *Chem. Eng. J.* **2010**, *164*, 29−36.
(82) Koriakin, A.; Ponvel, K. M.; Lee, C.-H. *Chem. Eng. J.* **2010**, *162*, 649−655.